



Hexagonal boron nitride epitaxial layers as neutron detector materials

J. Li, R. Dahal, S. Majety, J.Y. Lin, H.X. Jiang*

Department of Electrical and Computer Engineering, Texas Tech University, Lubbock, TX 79409, United States

ARTICLE INFO

Article history:

Received 23 May 2011

Received in revised form

19 July 2011

Accepted 20 July 2011

Available online 27 July 2011

Keywords:

Semiconducting hexagonal boron nitride

Solid-state neutron detectors

MOCVD growth

Epitaxial layers

ABSTRACT

Micro-strip metal–semiconductor–metal detectors for thermal neutron sensing were fabricated from hexagonal boron nitride (hBN) epilayers synthesized by metal organic chemical vapor deposition. Experimental measurements indicated that the thermal neutron absorption coefficient and length of natural hBN epilayers are about $0.00361 \mu\text{m}^{-1}$ and $277 \mu\text{m}$, respectively. A continuous irradiation with a thermal neutron beam generated an appreciable current response in hBN detectors, corresponding to an effective conversion efficiency approaching $\sim 80\%$ for absorbed neutrons. Our results indicate that hBN semiconductors would enable the development of essentially ideal solid-state thermal neutron detectors in which both neutron capture and carrier collection are accomplished in the same hBN semiconductor. These solid-state detectors have the potential to replace ^3He gas detectors, which faces the very serious issue of ^3He gas shortage.

© 2011 Elsevier B.V. All rights reserved.

Hexagonal boron nitride (hBN) possesses extraordinary physical properties and has emerged as an important material for deep ultraviolet photonics [1,2] and for the exploration of new physical properties in low dimensional systems similar to graphene [3,4]. Another potential application of hBN is in the area of solid-state neutron detectors. Neutron detectors with improved detection efficiency are highly sought for a range of applications, including fissile materials sensing, neutron therapy, medical imaging, the study of materials sciences, probing of protein structures, and oil exploration [5]. Currently, the highest efficiency for detecting fissile materials is accomplished using ^3He gas tubes. However, not only are ^3He tube based systems bulky, hard to configure, require high voltage operation, and difficult to transport via air shipment but also there is a significant shortage of ^3He gas [5]. Thus, there is an urgent need to develop solid-state neutron detectors.

The dominant approach for obtaining a solid-state detector currently is to coat boron containing neutron-to-alpha particle conversion material onto a semiconductor (such as on Si or GaAs) [6–9] or to construct a boron based semiconductor detector [10,11]. The working principle is that the boron-10 (^{10}B) isotope has a capture cross-section of 3840 b for thermal neutrons (with 0.025 eV energy), which is orders of magnitude larger than those of most isotopes [12,13]. When a ^{10}B atom captures a neutron, it undergoes the following nuclear reaction:



The efficiency of boron coated conversion devices is inherently low (2–5%) [6–9] since the two functions (neutron capture and electrical signal generation) occur in separate layers and there are conflicting thickness requirements of the converter layer—The boron (or boron containing) layer must be thick enough (tens of μm) to capture the incoming neutron flux, yet sufficiently thin (a few μm) to allow the daughter particles (α and Li) to reach into the semiconductor layer to generate electrons and holes because the range of α and Li particles from the reaction in ^{10}B is only around 2–5 μm [14]. While perforated semiconductor neutron detectors exhibited improved detection efficiency, there remain many design and optimization issues [7–9]. On the other hand, the efficiency of devices based on B_4C and pyrolytic boron nitride is still low, ranging from 1% to 7% [10,11]. Universally, this can be attributed to the following two issues: (a) material's porosity and disordered polycrystalline nature and (b) stringent requirement of large values of carrier diffusion length and lifetime. The boron layer has to be large (tens of μm) in order to capture a majority of the incoming neutron flux as well as to stop all the subsequent charged particles. This implies that the carrier lifetime, or equivalently the carrier diffusion length (L_D) has to be very long to enable the spatial separation of the electron–hole pairs before their recombination. Obtaining L_D on the order of tens of μm in any type of semiconductors grown by any technique is highly challenging.

The potential of hBN crystals for thermal neutron detection has recently been recognized [15,16]. It was shown that at similar dimensions, detectors fabricated from hBN microcrystals of natural composition embedded in a polystyrene binder matrix are more efficient than ^3He gas detectors [15]. Semiconducting hBN neutron detectors have not been previously realized, but are expected to

* Corresponding author. Tel.: +1 806 742 3533; fax: +1 806 742 1245.

E-mail addresses: jingyu.lin@ttu.edu (J.Y. Lin), hx.jiang@ttu.edu (H.X. Jiang).

possess all the wonderful attributes of semiconductor detectors as a result of the 50 years of R&D in semiconductor technologies. Here, we report the growth of hBN epilayers and the fabrication of a micro-strip planar metal–semiconductor–metal (MSM) detector to partially relax the requirement of long carrier lifetime and diffusion length for a solid-state neutron detector.

Hexagonal BN epitaxial layers of about 1 μm thickness were synthesized by metal organic chemical vapor deposition (MOCVD) using natural triethylboron (TEB) sources (containing 19.8% of ^{10}B and 80.2% of ^{11}B) and ammonia (NH_3) as B and N precursors, respectively. Prior to epilayer growth, a 20 nm BN or AlN buffer layer was first deposited on sapphire substrate at 800 $^\circ\text{C}$. The typical hBN epilayer growth temperature was about 1300 $^\circ\text{C}$. X-ray diffraction (XRD) was employed to determine the lattice constant and crystalline quality of the epilayers. XRD θ – 2θ scan revealed a c -lattice constant ~ 6.67 \AA , which closely matches the bulk c -lattice constant of hBN ($c=6.66$ \AA) [16–18], affirming that BN films are of a single hexagonal phase. Fig. 1 shows an XRD rocking curve of the (0 0 2) reflection of a 1 μm thick hBN film that possesses a full width at half maximum ($\sim 385''$) that is comparable to that of a typical GaN epilayer grown on sapphire with a similar layer thickness [19], revealing a relatively high crystalline quality of the MOCVD grown hBN epilayers. Secondary ion mass spectrometry (SIMS) measurement (performed by EAG Lab—Evans Analytical Group) revealed that hBN epilayers have excellent stoichiometry [2]. Undoped hBN epilayers typically have an electrical resistivity of $\sim 10^{13}$ Ω cm. This makes them highly suited for the fabrication of MSM detectors with extremely low dark current.

Fig. 2(a) shows a schematic illustration of the MSM neutron detector. The fabrication procedures consisted of the following steps. First, photolithography was employed to define the micro-scale strips (5 $\mu\text{m}/5$ μm width/spacing) followed by pattern transferring using inductively coupled plasma dry etching to form micro-strips. A bilayer of 5 nm/5 nm (Ni/Au) was deposited using

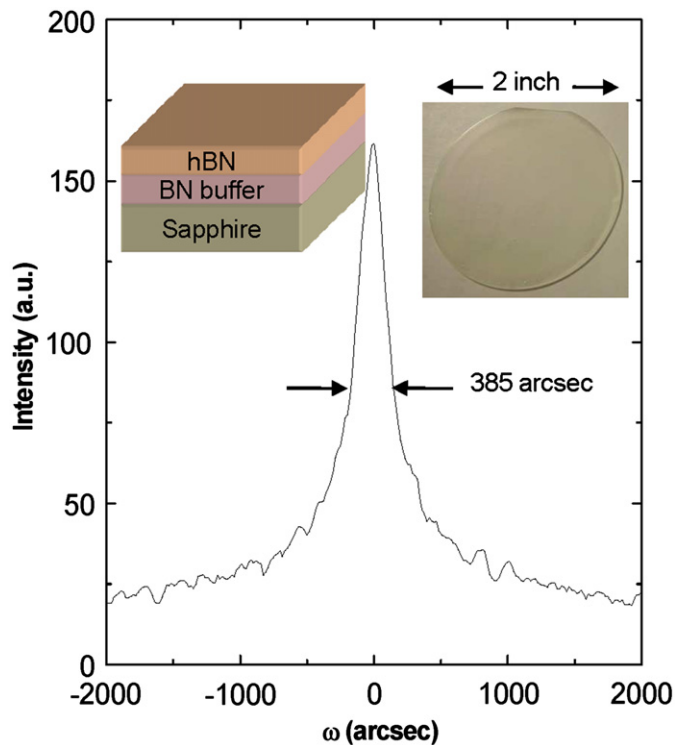


Fig. 1. XRD rocking curve of the (0 0 2) reflection of hBN. The insets are a schematic of the layer structure and an image of a 2-in. hBN epilayer wafer.

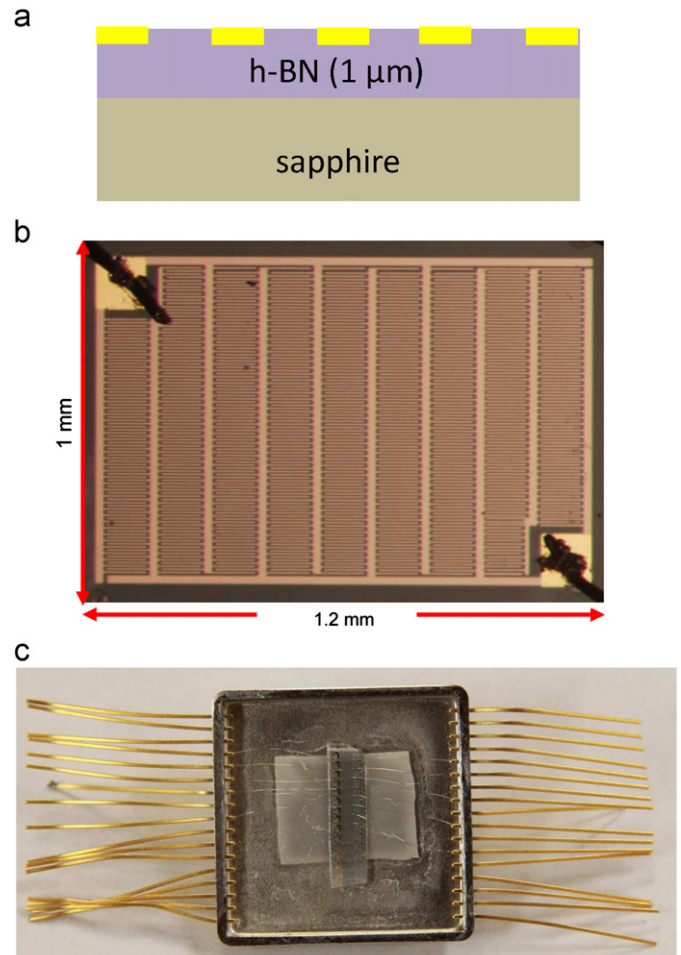


Fig. 2. (a) Illustration of hBN micro-strip MSM neutron detectors; (b) micrograph of a fabricated hBN micro-strip MSM neutron detector; and (c) micrograph of a packaged hBN micro-strip MSM neutron detector.

e -beam evaporation to form the Schottky contacts. Bonding pads were then formed by depositing an Au (200 nm) layer. Fig. 2(b) shows a finished device. The sapphire substrate was then polished and thinned to about 100 μm and diced to discrete devices, which were bonded onto device holders for characterization. An example of a bonded device is shown in Fig. 2(c). Preliminary measurements of interactions between neutrons and hBN materials were carried out at the Kansas State University TRIGA Mark II Reactor. The thermal neutron (0.025 eV) flux was set to about $6.2 \times 10^4/\text{cm}^2$ s for the experiment. The system for the steady current response measurements consisted of a source-meter and an electrometer connected in series.

Fig. 3(a) shows the measured attenuation of normal incidence thermal neutrons in hBN. In conducting the measurements, the variation in hBN epilayer thickness was accomplished by adding the number of hBN wafers in the thermal neutron beam path. Fitting experimental data by $I=I_0e^{-\alpha x}$ yields, respectively, an absorption coefficient (α) and absorption length (λ) of

$$\alpha = 0.00361 \mu\text{m}^{-1}$$

$$\lambda (= 1/\alpha) = 277 \mu\text{m}.$$

The microscopic thermal neutron absorption length can also be estimated by knowing the thermal neutron capture cross-section σ and density of ^{10}B in a hexagonal lattice of BN. We have

$$\sigma = 3.84 \times 10^3 \text{ b} = 3.84 \times 10^3 \times 10^{-24} \text{ cm}^2 = 3.84 \times 10^{-21} \text{ cm}^2$$

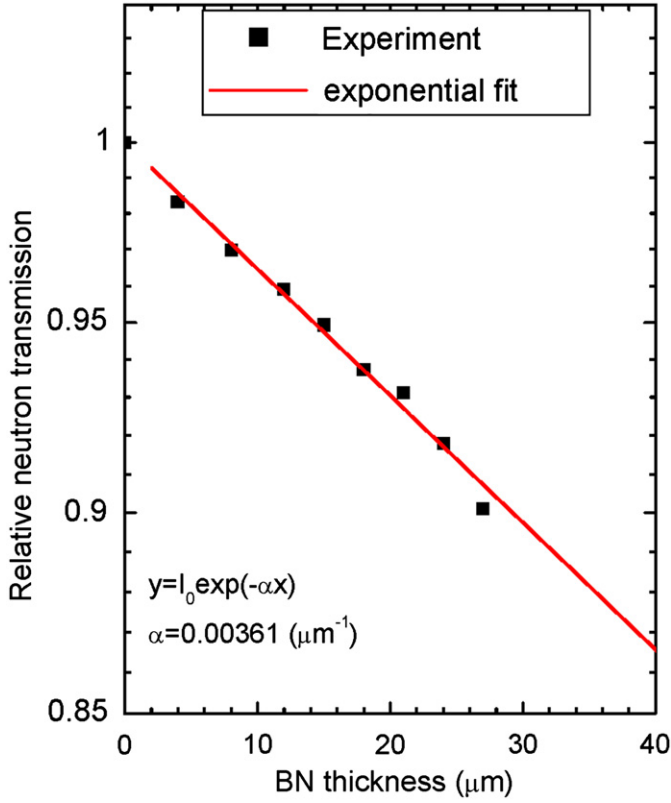


Fig. 3. Measured relative thermal neutron transmission in natural hBN epilayers.

A hexagonal lattice of BN has lattice constants of $a=2.50 \text{ \AA}$ and $c=6.66 \text{ \AA}$, which yields, respectively, the density for natural boron $N_{[B]}$ and ^{10}B isotope $N_{[B-10]}$ as

$$N_{[B]} = 5.5 \times 10^{22} \text{ cm}^{-3}$$

$$N_{[B-10]} = 20\%N_{[B]} = 1.1 \times 10^{22} \text{ cm}^{-3}.$$

These together yield a theoretical microscopic neutron absorption coefficient (Σ) and absorption length (λ) in a natural hBN as follows:

$$\Sigma = \sigma N_{[B-10]} = 3.84 \times 10^{-21} \text{ cm}^2 \times 1.1 \times 10^{22} \text{ cm}^{-3}$$

$$= 42 \text{ cm}^{-1} = 4.2 \times 10^{-3} \mu\text{m}^{-1}$$

$$\lambda = 1/\Sigma = 238 \mu\text{m}.$$

Thus, the estimated microscopic neutron absorption length is in close agreement with the measured value of $277 \mu\text{m}$.

The absolute current response of the detector to continuous irradiation of thermal neutron beam was measured. Although the neutron absorption layer in our devices was only $1 \mu\text{m}$, signal generation was evident. This is attributed to the unique planar micro-strip device architecture shown in Fig. 2 which not only effectively utilizes the outstanding lateral transport properties of hBN but also alleviates, to a certain degree, the stringent requirement of the large carrier diffusion length needed to ensure a maximum sweep out of electrons and holes at metal contacts. As illustrated in Fig. 4 it was found that the detectors have low background current and continuous irradiation by the thermal neutron beam at a flux of $6.2 \times 10^4/\text{cm}^2 \text{ s}$ generates a steady current response of about 0.085 pA , independent of the applied voltage in the measured range (20–100 V).

We can also estimate the carrier generation rate and magnitude of electrical current signal generated by the continuous irradiation of a thermal neutron beam by considering the dominant nuclear reaction described by Eq. (2). Based on the neutron

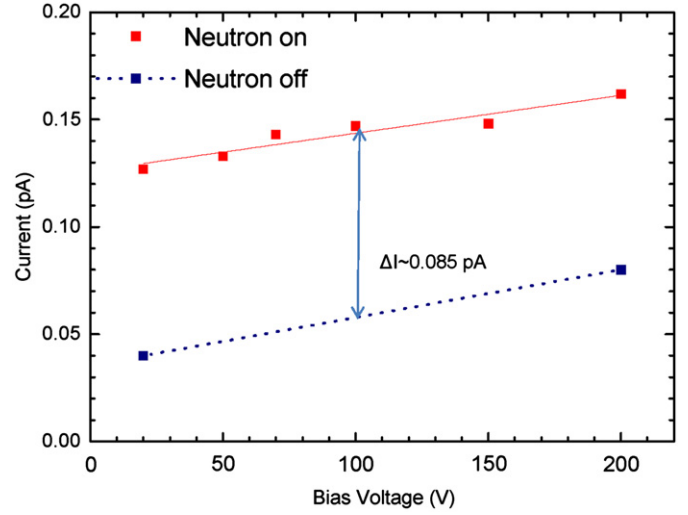


Fig. 4. Steady current response in an hBN micro-strip MSM detector ($1 \text{ mm} \times 1.2 \text{ mm}$) fabricated from an epilayer $1 \mu\text{m}$ in thickness, subjected to continuous irradiation with thermal neutron (0.025 eV) beam at a flux of $6.2 \times 10^4/\text{cm}^2 \text{ s}$.

beam flux (N_{flux}) used for the experiment, the measured neutron absorption length (λ), and device layer thickness ($t=1 \mu\text{m} \ll \lambda$), the effective absorbed neutron flux (N_{flux}^*) by the detector can be calculated and is

$$N_{\text{flux}}^* = (t/\lambda)N_{\text{flux}} = (1 \mu\text{m}/277 \mu\text{m}) \times 6.2 \times 10^4/\text{cm}^2 \text{ s}$$

$$= 2.2 \times 10^2/\text{cm}^2 \text{ s}.$$

On the other hand, the energy required to generate one electron–hole ($e^- - h^+$) pair is about three times the bandgap energy ($\sim 18 \text{ eV}$ in hBN) [12]. Based on the dominant nuclear reaction described by Eq. (2) each absorbed neutron is expected to generate daughter particles (Li and α) with kinetic energies of 2.310 MeV (94%) and 2.792 MeV (6%), giving an average energy of 2.34 MeV , or equivalently $1.3 \times 10^5 e^- - h^+$ pairs ($=2.34 \text{ MeV}/18 \text{ eV}$). Therefore, the free electron generation rate (n) would be $n=N_{\text{flux}}^* \times 1.3 \times 10^5$, or

$$n = 2.2 \times 10^2/\text{cm}^2 \text{ s} \times 1.3 \times 10^5 = 2.9 \times 10^7/\text{cm}^2 \text{ s}.$$

The magnitude of response current (I) can be estimated by knowing the device area ($A=1.2 \text{ mm}^2=1.2 \times 10^{-2} \text{ cm}^2$) as

$$I = 2 \times 2.9 \times 10^7/\text{cm}^2 \text{ s} \times 1.2 \times 10^{-2} \text{ cm}^2 (e) = 7.0 \times 10^5 \times 1.6$$

$$\times 10^{-19} (\text{A}) \sim 1.1 \times 10^{-13} (\text{A})$$

where the factor of 2 accounts for both the electron and hole conduction. Thus, the expected current of 0.11 pA is in accordance with the experimentally measured result of 0.085 pA . This close agreement between the expected and measured response currents not only provides high confidence in the measurement results, but also implies that the measured performance of the detector is at 77% ($=0.085/0.11$) of the theoretically predicted.

Since research of semiconducting hBN solid-state neutron detectors is in its very early stage, many issues merit further studies. These include methods to provide discrimination of neutrons from gamma radiation; conducting the neutron detection experiments in vacuum to further confirm the device indeed detects the neutrons as a semiconductor; and increased neutron absorption via increased epilayer thickness. An effective way to gain neutron detection efficiency is by ^{10}B isotopic enrichment of the source molecule, which can increase the neutron capture efficiency with little impact on the semiconducting properties. The use of a ^{10}B enriched ($100\% \text{ }^{10}\text{B}$) TEB source for B precursor will reduce the epilayer thickness requirement by a factor of 5.

Table 1
Comparison of ^3He gas detector, scintillation detector, and the proposed BN detector for thermal neutron sensing.

	^3He gas detector	Scintillation detector	B Coated detector	BN semiconductor detector
Particle generated by neutron	Ions	Photons	Ions, electrons, holes	Ions, electrons, holes
Active thickness	~ 10 cm	~ 1 mm	~ 100 μm	~ 100 μm
Key issue	Shortage of ^3He gas	Sensitivity	Sensitivity	Availability of suitable materials
Response speed	~ 1 ms	1 ns	1 ns	1 ns
Mechanism	$\text{He}^3 + n \rightarrow e^- + \alpha$ $e^- \rightarrow \text{Me}^-$	$n \rightarrow M(h\nu)$ $M \sim 10^5$	$\text{B} + n \rightarrow \text{Li} + \alpha$ $\text{Li}, \alpha \rightarrow \text{N}(e^-) + \text{N}(h^+)$ $N \sim 10^6$	$\text{B} + n \rightarrow \text{Li} + \alpha$ $\text{Li}, \alpha \rightarrow \text{N}(e^-) + \text{N}(h^+)$ $N \sim 10^6$
Intrinsic detection efficiency	High	Low	Low	High
Cost	High	Medium	Low	Low
Portability	Poor	Medium	High	High

This means that 200 μm thick ^{10}B enriched hBN epilayer can capture 98.5% of neutrons instead of 1 mm thickness required for natural hBN. However, with the existing semiconductor detector technology developed in the last 50 years, hBN based semiconductor neutron detectors have the potential to revolutionize neutron detection. With BN neutron capture, charge collection, and electrical signal generation occurring in a single material, the signal loss that is inherent in current existing solid-state detectors can be eliminated. The advantages of hBN semiconductor neutron detectors are summarized and compared to other detectors in Table 1. With further developments in material growth and device design such as incorporating thick ^{10}B enriched epilayers (or multiple ^{10}B enriched epilayers) with improved crystalline quality and device architectures to effectively utilize lateral transport in hBN, in principle, the neutron detection efficiency of hBN semiconductor detectors can approach 100%. Furthermore, the ability of producing wafer scale hBN semiconducting materials by techniques such as MOCVD also opens the possibility to construct relative large area detectors as well as two-dimensional array neutron cameras.

The neutron detector work is supported by DHS/NSF ARI Program (CBET-1038700 managed by Dr. Mark Wrobel). Epitaxial growth of hBN work is also supported in part by DRAPA-CMUVT (managed by Dr. John Albrecht). The authors are grateful to Dr. Jeffrey Geuther for his help with the neutron detection experiment and coordination with the Kansas State University TRIGA Mark II Reactor facility. Jiang and Lin are grateful to the AT&T Foundation for the support of Ed Whitacre and Linda Whitacre Endowed chairs.

References

- [1] Y. Kubota, K. Watanabe, O. Tsuda, T. Taniguchi, *Science* 317 (2007) 932.
- [2] R. Dahal, J. Li, S. Majety, B.N. Pantha, X.K. Cao, J.Y. Lin, H.X. Jiang, *Appl. Phys. Lett.* 98 (2011) 211110.
- [3] D. Pacilé, J.C. Meyer, Ç.Ö. Girit, and A. Zettl, *Appl. Phys. Lett.* 92 (2008) 133107.
- [4] L. Song, L. Ci, H. Lu, P.B. Sorokin, C. Jin, J. Ni, A.G. Kvashnin, D.G. Kvashnin, J. Lou, B.I. Yakobson, P.M. Ajayan, *Nano Lett.* 10 (2010) 3209.
- [5] R.T. Kouzes, J.H. Ely, L.E. Erikson, W.J. Kernan, A.T. Lintereur, E.R. Siciliano, D.L. Stephens, D.C. Stromswold, R.M. VanGinhoven, M.L. Woodring, *Nucl. Instr. and Meth. A* 623 (2010) 1035.
- [6] A. Rose, *Nucl. Instr. Meth. A* 52 (1967) 166.
- [7] D.S. McGregor, S.M. Vernon, H.K. Gersch, S.M. Markham, S.J. Wojtczuk, D.K. Wehe, *IEEE Trans. Nucl. Sci.* NS-47 (2000) 1364.
- [8] R.J. Nikolića, C.L. Cheung, C.E. Reinhardt, T.F. Wang, in: J. Piprek (Ed.), *Proceedings of SPIE, Optoelectronic Devices: Physics, Fabrication, and Application II*, vol. 6013, 2005, p. 601305.
- [9] J.K. Shultis, D.S. McGregor, *IEEE Trans. Nucl. Sci.* NS-53 (1659) 2006.
- [10] K. Osberg, N. Schemm, S. Balkir, J.O. Brand, M.S. Hallbeck, P.A. Dowben, M.W. Hoffman, *IEEE Sensors J* 6 (2006) 1531.
- [11] D.S. McGregor, T.C. Unruh, W.J. McNeil, *Nucl. Instr. and Meth. A* 591 (2008) 530.
- [12] G.F. Knoll, *Radiation Detection and Measurement*, 4th edition, John Wiley & Sons, 2010.
- [13] O. Osberghaus, *Z. Phys.* 128 (1950) 366.
- [14] F.P. Doty, Boron nitride solid-state neutron detector, US Patent 6727504.
- [15] J. Uher, S. Pospisil, V. Linhart, M. Schieber, *Appl. Phys. Lett.* 90 (2007) 124101.
- [16] V. Siklitsky, Boron Nitride, <<http://www.ioffe.rssi.ru/SVA/NSM/Semicond/BN/index.html>>.
- [17] S.L. Romyantsev, M.E. Levinshtein, A.D. Jackson, S.N. Mohammad, G.L. Harris, M.G. Spencer, M.S. Shur, in: M.E. Levinshtein et al. (Ed.), *Properties of Advanced Semiconductor Materials GaN, AlN, InN, BN, SiC, SiGe*, John Wiley & Sons, Inc., New York, 2001, pp. 67–92.
- [18] R.W. Lynch, H.G.J. Drickamer, *J. Chem. Phys.* 44 (1966) 181.
- [19] S. Nakamura, G. Fasol, S.J. Pearton, *The Blue Laser Diode: The Complete Story*, Springer, New York, 2000.